Theoretical study on performance of heterojunction solar cell using wide bandgap metal oxide semiconductors

SYED ZULQARNAIN HAIDER[a], SAFDAR IQBAL[a], HAFEEZ ANWAR[a,*], AHMAD GHADAFI ISMAIL[b], JAZIB ALI[c]
[a]*Department of Physics, University of Agriculture, 38040 Faisalabad, Pakistan*
[b]*Institute of Microengineering and Nanoelectronics, National University of Malaysia, Malaysia.*
[c]*School of Physics and Astronomy, and Collaborative Innovation Center of IFS (CICIFSA), Shanghai Jiao Tong University, 200240 Shanghai, China*

A device model is designed for cuprous oxide (Cu_2O) and zinc oxide (ZnO) based heterojunction solar cell. In this work, PC1D is used to analyze the recombination and transport mechanism of charge carriers considering the effect of thickness and doping concentration (N_A) of Cu_2O and ZnO on performance of the device. It is noted that Cu_2O has dominant influence on the performance of device as compared to ZnO. Power conversion efficiency (PCE) attains maximum value about 4 % and 3.68 % at thickness of 420 μm and N_A of 1×10^{16} cm^{-3} respectively.

(Received August 4, 2020; accepted November 24, 2021)

Keywords: Zinc oxide, Cuprous oxide, Heterojunction solar cell, Doping concentration, PC1D

1. Introduction

Energy from sun is recognized as suitable renewable energy to cope with worldwide energy demands [1]. Solar photovoltaics (PV) are critical for the conversion of solar radiation into electricity focusing on the material engineering of semiconductors [2–4]. Cu_2O with wide band gap (E_g) of 1.8-2.5 eV is an attractive optical absorber material due to low-cost, non-toxicity, easy synthesis, natural abundance for the production of pollution-free and sustainable low-cost PV devices as compared to other semi-conductor materials [5] that are also used in other applications such as organic diodes [6, 7] and transistors [8–10]. Cu_2O is a non-stoichiometric defect p–type semiconductor and its potential for the design of solar cells have been recognized since 1920. Cu_2O is a p-type metal oxide (MO) showing better hole mobility and stability [11]. Zinc oxide is wide direct bandgap n-type semi-conductor of 3.4 eV which is low cost, easy synthesis and high potential for use in optoelectronic and electronics due to transparency in visible spectral region. ZnO has with better match of transmission spectrum with absorption spectrum of Cu_2O. Furthermore, doping concentration influences the conductivity of semiconductors. The level of doping concentration decides the surplus valence electrons or vacant positions of valence electrons thus controlling the conductivity of semiconductors. It also allows the scientists to exploit the properties of materials which are used in the fabrication of solar cells [12]. Based on theoretical limit of efficiency (Shockley-Queisser), The PVs with single p-n junction with absorber layer of E_g (1.34 eV) have the maximum PCE of 33.77% [13]. Therefore, Cu_2O is attractive material to achieve this limit as compared to traditional semi-conducting material silicon (Si). The fabricated PVs had not achieved PCE as high as modeled PVs had achieved due to certain experimental limitations. This can also be explained by the fact that the concentrations of defects of materials and at PV interfaces have major influence on the film quality and PV performance [14]. The ability to modify the concentration of holes remains critical issue. However, high-target utilization sputtering (HiTUS) is used for the preparation of high-quality metal oxide (MO) thin films [15]. Cu_2O has shown its better applications as a strong optical absorber material in PVs [16]. Further, when light falls on semiconductor then it absorbs photons with energy greater than E_g, thus, excess charge carriers are generated which are then collected at the junctions [17]. Particularly, when E_g is very large then the high-energy photons are absorbed in the space charge region of a), the MO semiconducting layers are expected to perform well [18]. A detailed theoretical analysis would provide a suitable method for enhanced performance of PVs. Simulation methods are very important because these methods provide comprehensive and easy understanding of various physical phenomena of solar cells. These are various equations controlling and describing the different mechanism of solar cell. These equations are either solved numerically or analytically which is time consuming. Computer based solar cell simulation packages are used to solve these equations at high speeds with maximum accuracy [19, 20]. A finite element method (FEM) based PC1D is used to model one dimensional devices composed of various materials in accordance with various physical equations including Poisson equation and equation of continuity as well as transport equations [21–23]. In this study, a simulation tool PC1D is used to investigate the impact of thickness and doping concentration of MO materials on the PV

characteristics of heterojunction solar cell. The architecture ITO / ZnO / Cu_2O / Au is used for device and PV performance variation in accordance with the variation in thickness and doping concentration of ZnO and Cu_2O is analyzed. This work would provide theoretical basis for MO semiconductor suitable for PVs and for their enhanced performance in future.

2. Device architecture and simulation details

Theoretical analysis is as important as experimental analysis of the device in order to completely understand the different transport and recombination mechanisms in the device [24]. For theoretical analysis, device simulation is a powerful analytical technique for the testing and performance evaluation of device [25]. Therefore, device simulation of MO based PV with device structure ITO / ZnO / Cu_2O / Ag. The Cu_2O is used to replace conventional heterojunction layers (n-type Si, intrinsic-Si, p-type Si) in suitable device architecture. The influences of n-type and p-type MO on the PV properties of heterojunction devices are studied. The CBO and VBO are very crucial for efficient transport of holes and electrons across interfaces of device and controlling recombination rates [26]. Fig. 1 shows the nature of conduction band offset (CBO) and valence band offset (VBO). When conduction band minimum (CBM) of buffer is higher than that of absorber as shown in Fig.1a then energy barrier is created at the interface for the flow of electrons thus forming energy spike and CBO is positive. When valence band maximum (VBM) of buffer is higher than that of absorber as shown in Fig.1b then energy barrier is created at the interface for the flow of holes thus forming energy spike and VBO is negative. On the other hand, when conduction band minimum (CBM) of buffer is lower than that of absorber as shown in Fig. 1b then no energy barrier is created at the interface for the flow of electrons thus forming energy cliff and CBO is positive. The schematic structure diagram and band diagram are shown in Figs. 2a and b respectively. The CBM of ZnO lies below CBM of Cu_2O having CBO of -0.77 eV. The valence band maximum (VBM) of ZnO lies below VBM of Cu_2O having VBO of +1.97 eV.

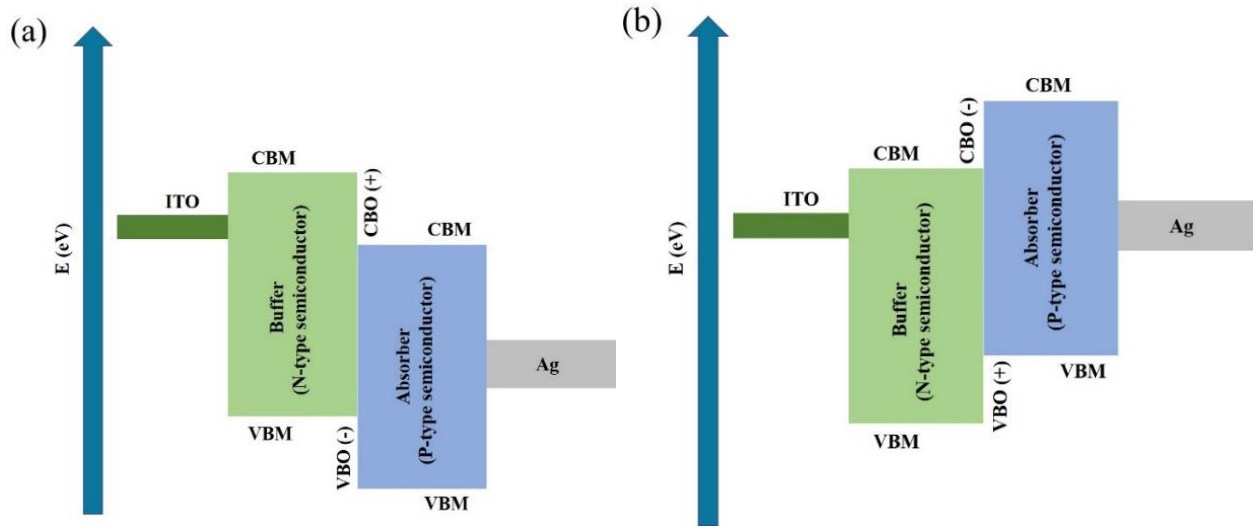

Fig. 1. Band alignment diagram of buffer / absorber interface (a) CBO(+)and VBO(-) (b) CBO(-)and VBO(+) (color online)

The simulation parameters of materials for theoretical analysis are listed in Table 1. Device simulation is carried out by considering only band to band recombination with no bulk defect having speed 10 cm/s at interfaces. The total area of the device was 10 cm^2. The front surface texture depth is 9 µm while front surface charge is set to 0. The front and back surface reflectance is considered as 5 % and 100 % respectively. The substrate thickness is set to be 0.12 µm. The front and back surface recombination rate is chosen as 10^3 cm/s and 10^5 cm/s respectively. The simulation is carried out under AM 1.5 illumination at 300 K. The sweep voltage is selected as -0.8 V to +0.8 V.

Table 1. Parameters of various materials used in device simulation [27–39]

Parameters	ITO	ZnO	Cu_2O
Thickness (μm)	0.12	0.2	170
Electron affinity χ (eV)	3.6	3.97	3.20
Band gap energy E_g (eV)	3.7	3.4	2.1
Relative permittivity ε_r	5.47	8.75	5.7
Effective conduction band density N_c (cm^{-3})	2.0×10^{18}	1×10^{18}	2.2×10^{18}
Effective valance band density N_v (cm^{-3})	1.8×10^{19}	1.3×10^{19}	1.8×10^{19}
Electron mobility μ_n ($cm^2 V^{-1}s^{-1}$)	1170	100	200
Hole mobility μ_p (cm^2 $V^{-1}s^{-1}$)	434.7	30	80
Donor concentration N_D (cm^{-3})	1×10^{16}	1×10^{16}	0
Acceptor concentration N_A (cm^{-3})	0	0	1×10^{16}
Refractive index	2.25	2.37	1.60

PC1D is based on the differential equations for device simulation of planar heterojunction solar cell as follows.

$$-\frac{d}{dx}\left(\frac{d\varphi}{dx}\right) = \frac{dE}{dx} = \frac{e}{\varepsilon\varepsilon_o}\left(p - n + N_n^+ - N_p^- - n_{trap} + p_{trap}\right) \quad (1)$$

$$\frac{1}{e}\left(\frac{dj_n}{dx}\right) = P(E)G - (1 - P(E)\alpha(np - n_i^2) \quad (2)$$

$$\frac{1}{e}\left(\frac{dj_p}{dx}\right) = P(E)G - (1 - P(E)\alpha(np - n_i^2) \quad (3)$$

$$j_n = en\mu_n E + \mu_n k_B T\frac{dn}{dx} \quad (4)$$

$$j_p = ep\mu_p E - \mu_p k_B T\frac{dp}{dx} \quad (5)$$

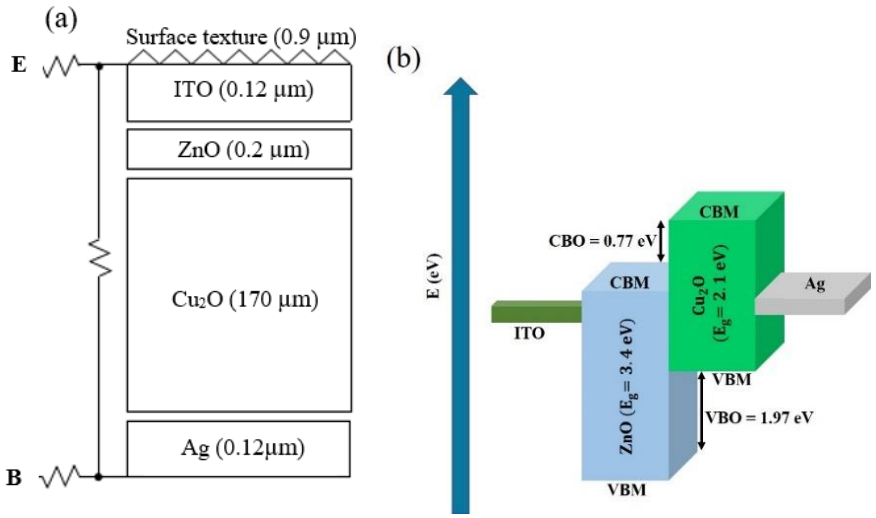

Fig. 2. (a) Structure of device (b) band diagram of device (color online)

Equation (1) represents the electric field and electric potential which depends on the space charge and doping. Equations (2-5) are current continuity equation represent the charge generation and recombination processes of electrons and holes. G and P(E) are the bound exciton generation rate and probability of dissociation of bound exciton respectively while n_i is the intrinsic carrier concentration. Recombination rate α is given by

$$\alpha = \frac{e}{\varepsilon\varepsilon_o}(\mu_n + \mu_p) \quad (6)$$

μ_n and μ_p are the electron and hole mobility respectively, while j_n and j_p represent the drift and diffusion current density respectively. It is assumed that diffusion obeys the Einstein relation and diffusivity is proportional to k_BT, k_B=1.38 ×10^{23} J/K and is Boltzmann constant. The total current density is given by

$$J = j_n + j_p \quad (7)$$

3. Results and discussion

The current density-voltage (J-V) and quantum efficiency (QE) curve has been drawn with simulation parameters given in Table 1 and shown in Fig. 3a and b respectively. Fig. 2b shows the absorbance of wavelength in absorber layer which is maximum in the range 450 nm to 550 nm in the visible region with onset at 660 nm. Further, Short circuit current density (J_{sc}) of 6.389 mA/cm^2, open circuit voltage (V_{oc}) of 0.6825 V, fill factor (FF) of 83.38 % and power conversion efficiency (PCE) of 3.635% are obtained. The simulated device performance and experimental results are consistent for MO based heterojunction solar cell [40]. Table 2 shows the consistency of simulation and experimental results.

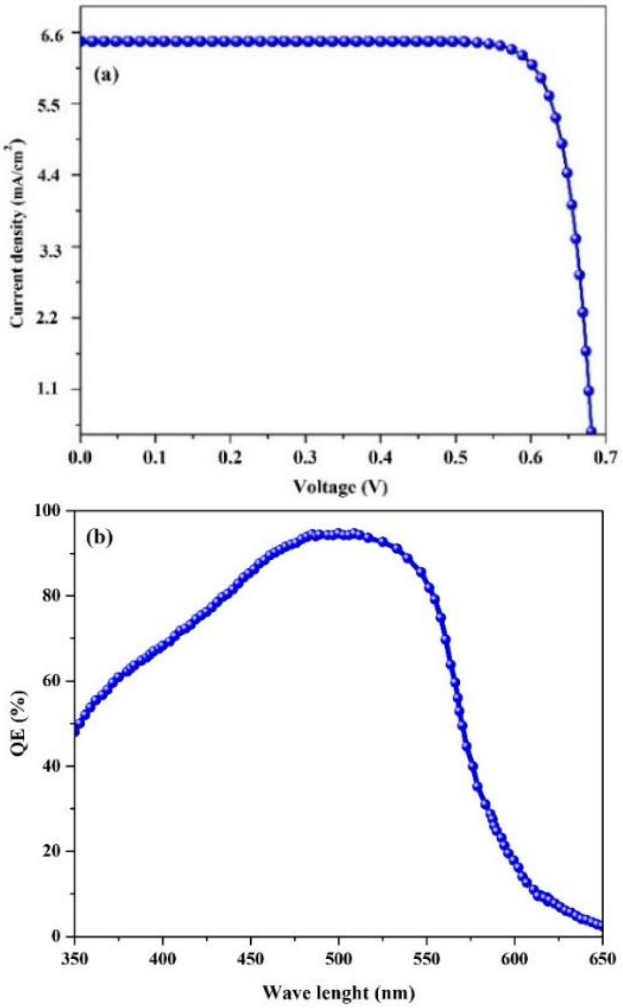

Fig. 3. Simulated (a) J-V curve (b) QE curve of the device (color online)

Table 2. Comparison of experimental and simulated results

Nature of work	J_{sc} (mA/cm^2)	V_{oc} (Volts)	FF (%)	PCE (%)
Experimental [40]	7.48	0.557	52.9	3.17
Simulation	6.389	0.6825	83.38	3.635

This consistency shows that input parameters are valid and close to real device.

3.1. Effect of thickness of Cu_2O and ZnO layers

Light absorber layer is very crucial influencing the fabrication cost and performance of the PVs. As long lifetime of the electrons and holes generated in the Cu_2O layer with high optical absorption coefficient (10^5 cm^{-1}) essentially ensures the large photocurrent of the PVs [41, 42]. The low photons having energy less than E_g passes through optical window of device whereas photons energies greater than E_g are absorbed in the wide-bandgap n-type material. In this study, the thickness of the n-type ZnO layer and p-type Cu_2O layer is varied from 0.2 µm to 1.2 µm and 170 µm to 620 µm respectively. The variation in performance parameters of the device with thickness of Cu_2O and ZnO are shown in Fig. 4a and b. J_{sc} and PCE curves show very similar behaviors with the increase in the thickness of Cu_2O as shown in Fig. 4a, J_{sc} and PCE increase rapidly when thickness increases from 175 µm to 375 µm. This is due to the fact that PV performance increases with the increasing thickness of the absorber layer and thus providing large cross-section to sunlight [43]. With further increase in thickness of Cu_2O layer, there is very little increase of both J_{sc} and PCE and nearly show a stable behavior. FF increases with the increase in thickness of Cu_2O up to 375 µm then begins to decrease due to increase in shunt resistance. V_{oc} exhibits almost stable behavior with the increase in thickness of Cu_2O. It is evident that 375 µm is the optimum thickness of Cu_2O for enhanced performance of the device. These results indicate that thicker layer of absorber material have minor influence enhancing on the performance of device. As well as the thickness of ZnO is concerned, very little effect is observed in the performance of the device with the increase in thickness of ZnO. PCE, J_{sc} and FF increase very slowly and attain maximum value when thickness is 0.6 µm and show stable behavior beyond this thickness of ZnO. On the contrary, V_{oc} shows a decrease when thickness of ZnO is 0.6 µm and then becomes stable. Based on these results, the optimum thickness of ZnO is found to be 0.6 µm.

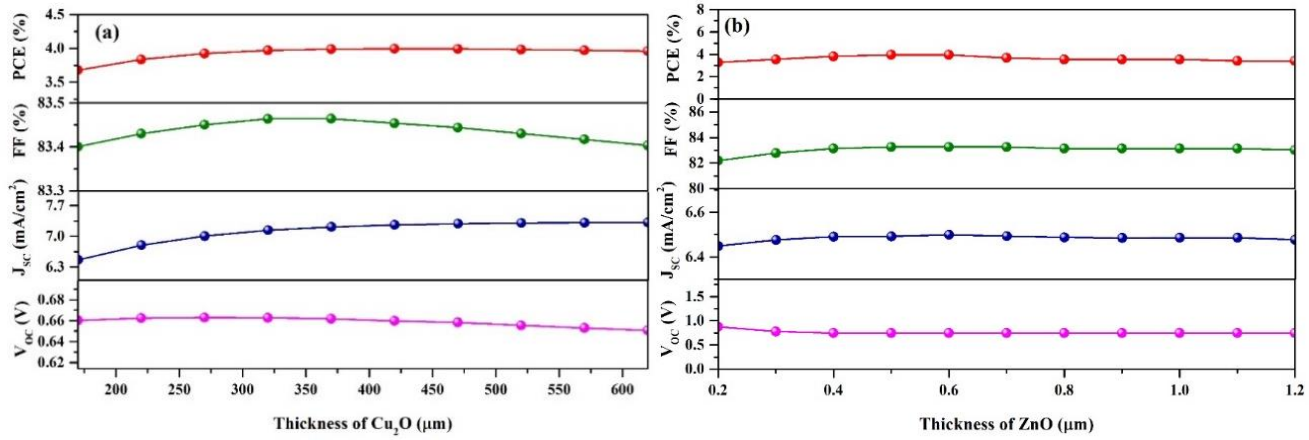

Fig. 4. Variation in performance parameters of device with thickness of (a) Cu_2O layer (b) ZnO layer (color online)

3.2. Effect of doping concentration of Cu_2O and ZnO layers

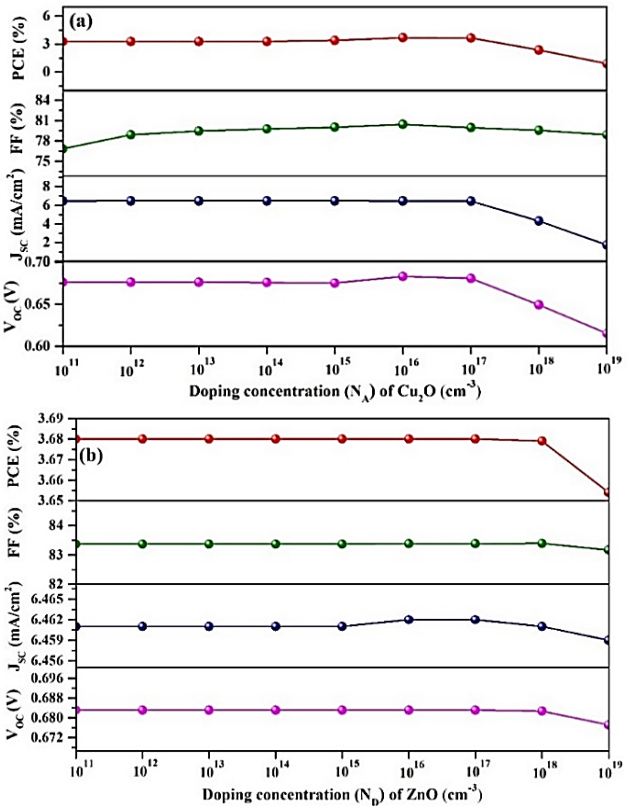

Fig. 5. Variation in performance parameters of device with doping concentration of (a) Cu_2O layer (b) ZnO layer (color online)

Doping of a material is very important parameter to change the properties of material and performance of a device. In general, a material can be doped in two different ways such as n-type doping and p-type doping [44]. The main purpose of doping is to increase the charge carriers which are readily available for the conduction within the material and across the whole device. There are various techniques which are used to dope the materials including successive ionic layer adsorption and reaction (SILAR) method, chemical co-precipitation method, pulsed laser deposition method [45–47]. The optimum doping concentration can enhance the performance of device. In this study, the effect of various doping concentration Cu_2O and ZnO is analyzed. Fig. 5a and b shows the variation in performance of device with the doping concentration of Cu_2O and ZnO respectively. PCE and J_{sc} show almost stable behavior when N_A of Cu_2O is changed from 1×10^{11} cm^{-3} to 1×10^{15} cm^{-3} and increased from 1×10^{15} cm^{-3} to 1×10^{17} cm^{-3}. Beyond 1×10^{17} cm^{-3}, PCE and J_{sc} begin to decrease thus showing deteriorating behavior as shown in Fig. 5a. V_{oc} and FF also exhibit almost the same behavior. The main reason of degradation of performance with high value of doping concentration is high recombination rate of excess charge carrier with the material and at interfaces. From these results, it is concluded that, 1×10^{16} cm^{-3} is optimum N_A of Cu_2O for better performance of the device. Fig. 4b shows the variation in performance of device with the increasing doping concentration of ZnO. PCE and J_{sc} show almost stable behavior when N_D of ZnO is changed from 1×10^{11} cm^{-3} to 1×10^{16} cm^{-3} and increased from 1×10^{16} cm^{-3} to 1×10^{17} cm^{-3}. Beyond 1×10^{17} cm^{-3}, PCE and J_{sc} begin to decrease thus showing deteriorating behavior as shown in Fig. 5b. V_{oc} and FF also exhibit almost the same behavior. From these results, it is concluded that, 1×10^{17} cm^{-3} is optimum doping concentration of ZnO for better performance of the device.

4. Conclusion

In this paper, ITO / ZnO / Cu_2O / Ag heterojunction solar cell was studied by using PC1D simulation software. The effect of thickness and doping concentration of the light absorber layer (Cu_2O) and window layer (ZnO) on performance of heterojunction device were investigated. It was noted that Cu_2O thickness had more influence on the device performance than ZnO thickness. The results show that moderate thickness of Cu_2O (375 μm) leads towards better device performance identifying strong sunlight absorbing capability of Cu_2O. The optimum thickness of ZnO layer was estimated as 0.6 μm for better performance and inhibiting the charge carrier recombination as well as

suitable transmission of wave lengths. Another important parameter, doping concentration, was also studied and its effect on device performance was investigated. Results show that doping concentration of absorbing layer and window layer have significant effect on device performance. Optimum doping concentration for absorber and window layer were found to be 1×10^{17} cm^{-3} and 1×10^{16} cm^{-3} respectively. This study provides a theoretical basis for MO semiconductors as PVs highlighting the solution for problems in fabrication of efficient devices.

Acknowledgements

Authors acknowledge the funding from Higher Education Commission, Pakistan for National Research Programme for Universities (NRPU) [Project number 8545] Ministry of Higher Education Malaysia [FRGS/1/2018/TK04/UKM/02/11] and National University of Malaysia [GUP-2018-158].

References

[1] P. A. Owusu, S. Asumadu-Sarkodie, Cogent Engineering **3**, 1 (2016).
[2] H. L. Tuller, Mater. Renew. Sustain. Energy **6**, 1 (2017).
[3] S. A. Salleh, M. Y. A. Rahman, Z. Yumni, T. H. T. Aziz, Arab. J. Chem. **13**, 5191 (2020).
[4] S. N. Sadikin, M. Y. A. Rahman, A. A. Umar, Optik **211**, 6 (2020).
[5] S. McWilliams, C. D. Flynn, J. McWilliams, D. C. Arnold, R. A. Wahyuono, A. Undisz, M. Rettenmayr, A. Ignaszak, Nanomaterials **9**, 1 (2019).
[6] K. Myny, S. Steudel, P. Vicca, J. Genoe, P. Heremans, Appl. Phys. Lett. **93**, 093305 (2008).
[7] S. Steudel, K. Myny, V. Arkhipov, G. Deibel, S. de Vusser, J. Genoe, P. Heremans, Nat. Mater. **4**, 597 (2005).
[8] A. G. Ismail, Org. Electron. **56**, 111 (2018).
[9] A. G. Ismail, Mater. Focus. **7**, 480 (2018).
[10] A. G. Ismail, I. G. Hill, Org. Electron. **12**, 1033 (2011).
[11] S. Chatterjee, A. J. Pal, J. Phys. Chem. C. **120**, 1428 (2016).
[12] H. Abedini-Ahangarkola, S. Soleimani-Amiri, Int. J. Eng. Trans. A Basics **34**, 873 (2021).
[13] M. H. Elshorbagy, B. García-Cámara, E. López-Fraguas, R. Vergaz, Nanomaterials. **9**, 1 (2019).
[14] J. H. Werner, J. Mattheis, U. Rau, Thin Solid Films **480**, 6 (2005).
[15] Z. Wang, P. K. Nayak, J. A. Caraveo-Frescas, H. N. Alshareef, Adv. Mater. **28**, 3831 (2016).
[16] T. Minami, Y. Nishi, T. Miyata, Appl. Phys. Express **9**, 1 (2016).
[17] Z. G. Ling, P. K. Ajmera, M. Anselment, L. F. Dimauro, Appl. Phys. Lett. **51**, 1445 (1987).
[18] S. Z. Haider, H. Anwar, Y. Jamil, M. Shahid, J. Phys. Chem. Solids. **136**, 1 (2020).
[19] S. Z. Haider, H. Anwar, S. Manzoor, A. G. Ismail, M. Wang, Curr. Appl. Phys. **20**, 1080 (2020).
[20] M. Goudarzi, M. Banihashemi, J. Photonics Energy **7**, 029901 (2017).
[21] G. Hashmi, M. J. Rashid, Z. H. Mahmood, M. Hoq, M. H. Rahman, J. Theor. Appl. Phys. **12**, 327 (2018).
[22] R. Sharma, Heliyon. **5**, 1 (2019).
[23] B. Hussain, A. Aslam, T. M. Khan, M. Creighton, B. Zohuri, Electron. **8**, 1 (2019).
[24] S. Z. Haider, H. Anwar, M. Wang, Semicond. Sci. Technol. **33**, 1 (2018).
[25] T. P. Morris, I. R. White, M. J. Crowther, Stat. Med. **38**, 2074 (2019).
[26] K. T. Butler, G. Sai Gautam, P. Canepa, Computational Materials **5**, 19 (2019).
[27] N. Zhang, J. Sun, H. Gong, Coatings. **9**, 1 (2019).
[28] F. Khaled, A. Bouloufa, K. Djessas, R. Mahamdi, I. Bouchama, Vacuum **120**, 14 (2015).
[29] B. Rajesh Kumar, B. Hymavathi, T. Subba Rao, Materials Today: Proceedings. Elsevier Ltd (2017).
[30] F. M. T. Enam, K. S. Rahman, M. I. Kamaruzzaman, K. Sobayel, P. Chelvanathan, B. Bais, M. Akhtaruzzaman, A. R. M. Alamoud, N. Amin, Optik **139**, 397 (2017).
[31] M. Y. X. Jiang, Solar Cells - Research and Application Perspectives, InTech (2013).
[32] H. Siddiqui, M. R. Parra, P. Pandey, N. Singh, M. S. Qureshi, F. Z. Haque, Orient. J. Chem. **28**, 1533 (2012).
[33] L. Zhu, G. Shao, J. K. Luo, Solid State Sci. **14**, 857 2012).
[34] F. A. Jhuma, M. Z. Shaily, M. T. Rashid, Mater. Renew. Sustain. Energy **8**, 1 (2019).
[35] M. A. M. Hassan, A. F. Saleh, S. J. Mezher, Appl. Nanosci. **4**, 695 (2014).
[36] Z. Liu, Y. Liu, X. Wang, W. Li, Y. Zhi, X. Wang, P. Li, W. Tang, J. Appl. Phys. **126**, 1 (2019).
[37] Z. Zang, Appl. Phys. Lett. **112**, 1 (2018).
[38] E. Afshari Pour, C. Shafai, Oxide-based Materials and Devices VIII. SPIE (Teherani, F.H., Look, D.C., and Rogers, D.J., eds.) (2017).
[39] A. S. Gadallah, M. M. El-Nahass, Adv. Condens. Matter Phys. **2013**, 1 (2013).
[40] G. Giorgi, J. I. Fujisawa, H. Segawa, K. Yamashita, J. Phys. Chem. Lett. **4**, 4213 (2013).
[41] T. K. S. Wong, S. Zhuk, S. Masudy-Panah, G. K. Dalapati, Materials **9**, 1 (2016).
[42] C. Jayathilaka, L. S. R. Kumara, K. Ohara, C. Song, S. Kohara, O. Sakata, W. Siripala, S. Jayanetti, Crystals **10**, 1 (2020).
[43] G. W. Kim, D. V. Shinde, T. Park, RSC Adv. **5**, 99356 (2015).
[44] S. Z. Haider, H. Anwar, M. Wang, Phys. Status Solidi **216**, 1 (2019).
[45] R. Shimizu, I. Sugiyama, N. Nakamura, S. Kobayashi, T. Hitosugi, AIP Adv. **8**, 1 (2018).
[46] P. P. Chandra, A. Mukherjee, P. Mitra, J. Mater. **2014**, 1 (2014).
[47] I. A. Kariper, Iran. J. Sci. Technol. Trans. A Sci. **40**, 137 (2016).

* Corresponding author: hafeez.anwar@gmail.com